MODELING THE EFFECT OF GRAIN BOUNDARY SLIDING ON CREEP LIFETIME: APPLICATION TO TWO AUSTENITIC STAINLESS STEELS.

Sivasambu Mahesh[a] and M. D. Mathew[b]

[a] Departments of Mechanical and Aerospace Engineering, Indian Institute of Technology, Kanpur.

[b]Mechanical Metallurgy Division, Indira Gandhi Centre for Atomic Research, Kalpakkam.

A model capable of representing the evolution rate of various damage mechanisms pertinent to creep rupture of austenitic stainless steels is utilized to study the role of grain boundary sliding on the damage evolution in the form of cavitational damage at grain boundary facets and wedge cracking at triple lines and on the creep lifetime of a standard creep specimen. Reduced grain boundary sliding reduces the rate of damage evolution and hence prolongs creep lifetime at higher stresses. However, creep lifetime at lower stresses is controlled by diffusional cavitation and remains unaffected by grain boundary sliding.

1. Introduction

At a fixed temperature, creep damage and eventual creep rupture of austenitic stainless steels are well-known to occur by a mechanism of grain boundary sliding assisted wedge cracking at triple points at moderate stresses. This failure mode transitions to a diffusional cavitation dominated failure mode at low stresses (1; 2). A model that represents the rate of evolution of the important damage mechanisms in austenitic stainless steels has been recently developed (3). In this model, the initial microstructure is idealized as a space-tiling aggregate of identical rhombic dodecahedral grains, which undergo power law creep deformation. Damage evolution in the form of cavitation and wedge-cracking on grain boundary facets is considered. Both diffusion- and deformation-driven grain boundary cavity growth are treated. Cavity and wedge-crack length evolution is derived from an energy balance argument that combines and extends the models of Cottrell, Williams and Evans.

Creep deformation in the model of ref. (3) follows the Norton power law, given by

$$\dot{\epsilon} = \left(\frac{\sigma}{\sigma_0}\right)^{n_a}.$$

This expression relates the strain rate, $\dot{\epsilon}$ to the equivalent stress, σ. σ_0 and n_a denote the reference stress and the creep exponent, respectively. Grain boundary sliding in four directions at each of the twelve facets of the rhombic dodecahedral grain are taken to follow the empirical law proposed by Horton (4):

$$\frac{\tau}{\sigma_0} = T_s\left(\frac{S}{S_0}\right)^{1/n_s} + T_a\left(\frac{S}{S_0}\right)^{1/n_a},$$

where, τ denotes the resolved shear stress on a grain boundary facet, which may cause grain boundary sliding at the rate of S. S_0 denotes the grain boundary sliding rate. The exponent n_s denotes the intrinsic exponent governing grain boundary sliding. Horton (4) has suggested a value of $n_a = 3.3$. T_s and $T_a$denote non-dimensional scaling parameters, which determine the intrinsic grain boundary resistance to sliding and the constraint offered by the surrounding matrix to a sliding grain boundary facet, respectively.

Diffusion driven cavitation in assumed to evolve following the model of Cocks and Ashby (5). A significant material parameter controlling the rate of diffusional cavities on grain boundary facets in this model is φ_1, whose variation with temperature in austenitic stainless steel has been studied by Smith and Gibbs.

2. Results and Discussion

It is the purpose of this article to apply the model of ref. (3) to two nuclear grade austenitic stainless steels, AISI 316 and alloy D9, which differ in their creep deformation characteristics and the characteristics of grain boundary sliding. Model parameters describing the two steels are given in the table below.

Parameter	**316 SS (873K)**	**D9 (973K)**
n_a	11	9.42
σ_0	166 MPa	170 MPa
T_s	0.301	0.059
T_a	0.163	0.235
φ_1	6×10^{-11}/MPa s	2.2×10^{-10}/MPa s

The dependence of the time to rupture on applied stress for both steels considered is well-captured by these parameters, as shown in Fig. 1. A sharp downward bend of the model predictions is observed in both materials, which corresponds to the transition from the regime of dominance of damage assisted by grain boundary sliding to the regime of dominance of cavitational damage. The dependence of grain boundary sliding rate on the resolved shear stress, given by Horton's formula above is also sketched for the parameters corresponding to the two materials in Fig. 2. It is clear from this figure that whereas at low normalized resolved shear

stress, $\frac{\tau}{\sigma_0} \leq 0.1$, the normalized sliding rate of both steels is approximately equal, for higher normalized resolved shear stress, the normalized sliding rate in the D9 alloy is greater than that in the 316 stainless steel.

The present model is also able to predict microstructural evolution of damage with time. Of the 12 facets of the regular rhombic dodecahedron idealizing a grain, two facets are normal to the tensile direction. These are called the normal facets. The other eight facets are inclined to the tensile direction, and are called inclined facets. By symmetry, damage evolves identically in both normal facets. Likewise damage evolves identically in the eight incline facets. Damage evolution with time for four applied stress levels has been shown for 316SS in Fig. 3 and for alloy D9 in Fig. 4. The left side column of these figures shows damage evolution in the normal facets and the right side column that in the inclined facets.

At the applied stress level of 225 MPa, creep rupture occurs in the 316SS specimen even before completion of damage accumulation in the inclined facets. This indicates a ductile or Hoff failure mode. In the alloy D9 specimens however, for the applied stress levels studied, the failure mode is always brittle: material failure occurs only after both normal and inclined facets become fully damaged. Figs. 3 and 4 show that damage evolution in the two materials is qualitative similar. The smaller rate of grain boundary sliding in 316SS at 873K than that in alloy D9 at 973K causes the creep lifetime of the former material to be longer than that of the latter at high stresses. In the low stress regime of the creep curve (85 MPa), however, the reason for the smaller creep lifetime of the D9 alloy than that of the 316SS is the higher rate of diffusional cavitation, caused by the higher value of φ_1 at higher temperatures.

References

1. Frost, H. J. and Ashby, M. F. *Deformation mechanism maps*: Pergamon, 1982.

2. Miller, D.A. and Langdon, T. G., Metal mater. trans., 10A (1979) 1635.

3. Mahesh, S, Alur, K. C and Mathew, M. D., Modelling Simul. Mater. Sci. Eng, 19 (2011) 015005.

4. Horton, C.A.P., *The interdependence between grain boundary sliding and grain creep deformation.* Proc. Bolton Landing conference. (1975) 355.

5. Cocks, A. C. F. and Ashby, M. F., *Prog. mater. sci.* 27 (1982) 189.

6. Smith, A. F and Gibbs, G. B., *Metal Sci. J.* 3 (1969) 93.

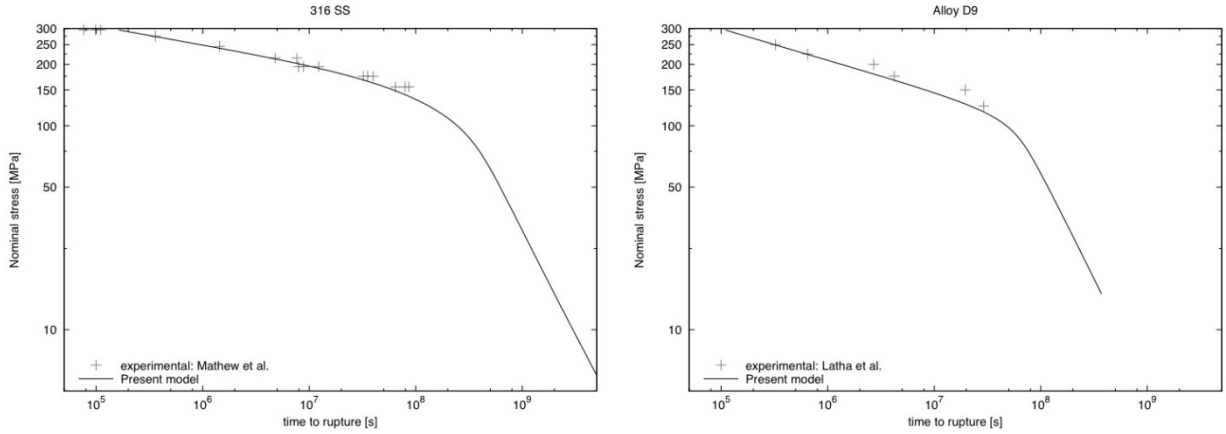

Figure 1: Comparison of the experimental and predicted time to rupture for 316 SS and alloy D9.

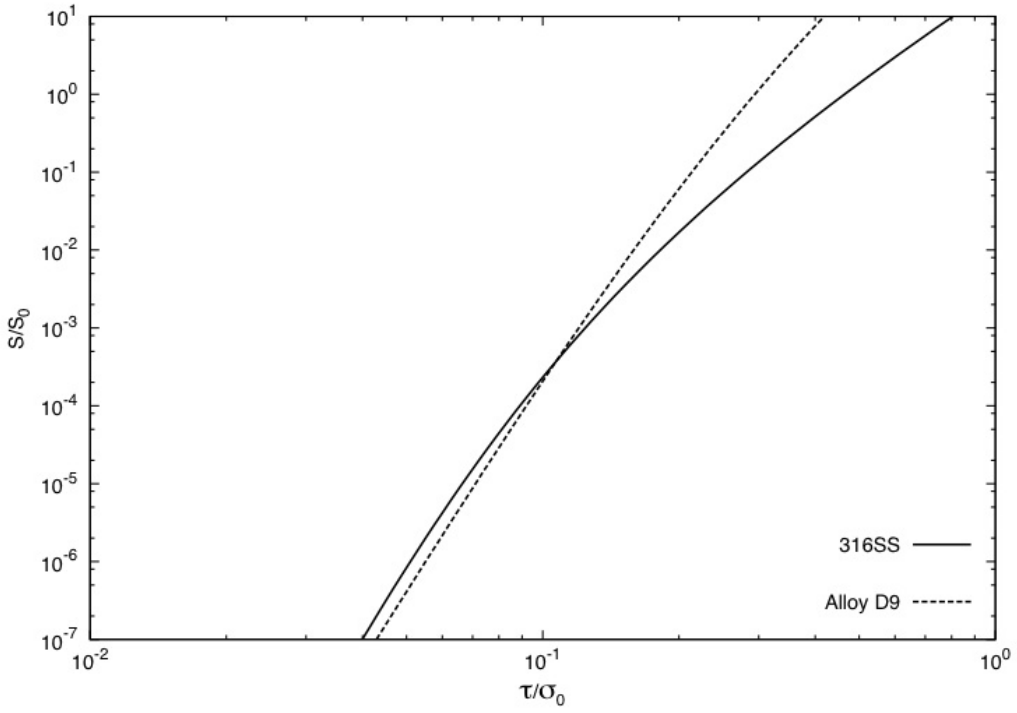

Figure 2: Variation of grain boundary sliding rate with resolved shear stress following Horton's formula. The testing temperatures are 873K for 316SS and 973K for alloy D9.

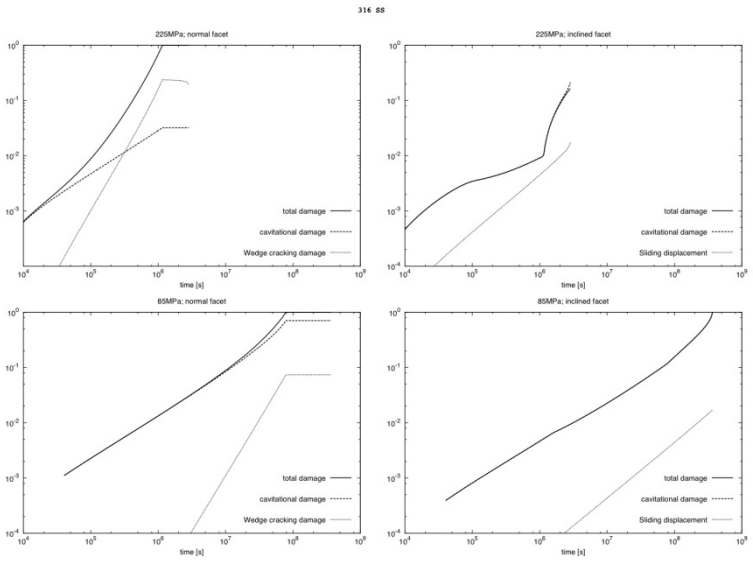

Figure 3: Evolution of damage in 316SS at two stress levels (225 MPa and 85 MPa) in the normal facets (left column) and in the inclined facets (right column).

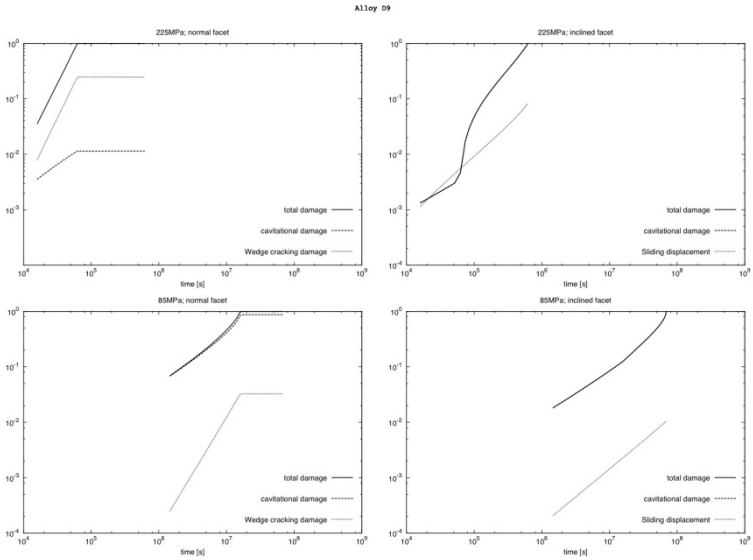

Figure 4: Evolution of damage in alloy D9 at two stress levels (225 MPa and 85 MPa) in the normal facets (left column) and in the inclined facets (right column).